

Synthesis and Biological Evaluation of *N*-Heterocyclic Indolyl Glyoxylamides as Orally Active Anticancer Agents

Wen-Tai Li,[†] Der-Ren Hwang,[†] Ching-Ping Chen,[†] Chien-Wei Shen,[†] Chen-Long Huang,[†] Tung-Wei Chen,[†] Chi-Hung Lin,[‡] Yee-Ling Chang,[†] Ying-Ying Chang,[†] Yue-Kan Lo,[†] Huan-Yi Tseng,[†] Chu-Chung Lin,[†] Jeng-Shin Song,[†] Hua-Chien Chen,[†] Shu-Jen Chen,[†] Se-Hui Wu,[†] and Chiung-Tong Chen^{*,†}

Division of Biotechnology and Pharmaceutical Research, National Health Research Institutes, 9F, 161, Sec. 6, Min-Chiuan East Road, Nei-Hu, Taipei 114, Taiwan, R.O.C., and Institute of Microbiology and Immunology, National Yang Ming University, Shih-Pai, Taipei 112, Taiwan, R.O.C.

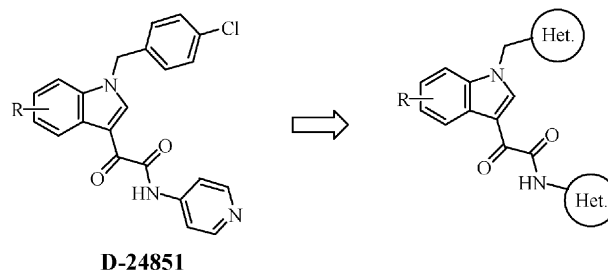
Received October 22, 2002

A series of *N*-heterocyclic indolyl glyoxylamides were synthesized and evaluated for in vitro and in vivo anticancer activities. They exhibited a broad spectrum of anticancer activity not only in murine leukemic cancer cells but also in human gastric, breast, and uterus cancer cells as well as their multidrug resistant sublines with a wide range of IC₅₀ values. They also induced apoptosis and caused DNA fragmentation in human gastric cancer cells. Among the compounds studied, **7** showed the most potent activity of growth inhibition (IC₅₀ = 17–1711 nM) in several human cancer cells. Given orally, compounds **7** and **13** dose-dependently prolonged the survival of animals inoculated with P388 leukemic cancer cells. *N*-Heterocyclic indolyl glyoxylamides may be useful as orally active chemotherapeutic agents against cancer and refractory cancerous diseases of multidrug resistance phenotype.

Introduction

The indole skeleton often appears in the natural products with a variety of biological activities.^{1–5} A number of clinical therapeutics such as indomethacin,⁶ indoramin,⁷ and indorenate⁸ also consist of an indole moiety. A newly discovered anticancer agent D-24851 (Chart 1) contains an indole glyoxylamide skeleton and possesses in vitro/in vivo anticancer activities.^{9–11} It was reported that isosteric substitutions with heterocycles often provides pharmacological and pharmacokinetic benefits as drug candidates for further development.^{12–15} Others have shown heterocycle substitutions may cause changes in the degree of ionization of compounds in physiological pH resulting in changes of their basicity and lipophilicity and thus substantial differences in pharmacokinetic properties.¹³ Furthermore, heterocycle substitutions of the phenyl, anilic, or an isosteric structure were reported of better pharmacological efficacy^{14,15} and pharmacokinetic properties,^{14,15} and less toxicity.¹⁴ A change in the orientation (positions of substitution) of the isoxazole ring changes the biological activity.¹² It would be interesting to know whether the replacements of the benzene rings with heterocyclic rings at 1- and/or 3-positions of the indolyl glyoxylamide skeleton may enhance their biological activities and provide benefits and the basis for further development as drug candidates. We report here the synthesis of a number of *N*-heterocyclic indolyl glyoxylamides and the evaluation of their biological activity of in vitro growth inhibition of cancer cells and in vivo prolongation of cancer survival in animals.

Chart 1



Chemistry

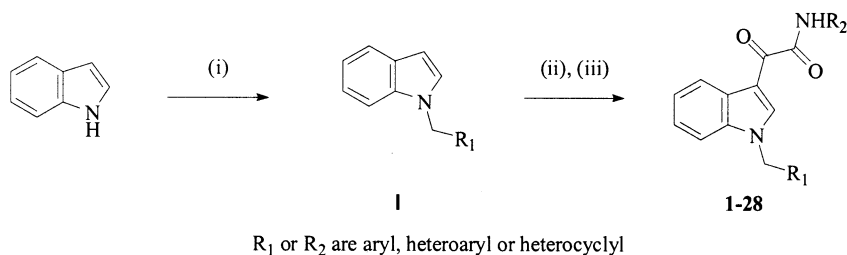
N-Substituted indolyl glyoxylamides **1–28** were synthesized according to the general synthetic approach shown in Schemes 1 and 2. According to Route I, the potassium salt of indole was chosen to react with an aralkyl halide to give the corresponding *N*-substituted product **I**.^{16–18} The use of Grignard reagent and sodium carbonate as bases was restricted, as indole undergoes preferential alkylation at the 3-position of indole.^{19,20} The aralkyl halides were prepared either via the halide substitution of an aralkyl alcohol^{21–23} or via a 1,3-dipolar addition reaction to generate the five-membered heterocyclic ring (**5–10**).²⁴ Reaction of the *N*-substituted indole with oxalyl chloride at nucleophilic 3-position of indole was facile at 0 °C. Subsequently, on treatment with a mild base such as triethylamine, the various *N*-substituted indoles underwent substitution reaction to give the desired products.

Alternatively, the indolyl glyoxylamides could also be synthesized by use of another methodology (Scheme 2, Route II). The treatment of indole with oxalyl chloride produced 2-(1*H*-3-indolyl)-2-oxoethanoyl chloride due to the high nucleophilic character at 3-position of indole,^{25,26} and intermediate **II** was then produced by a

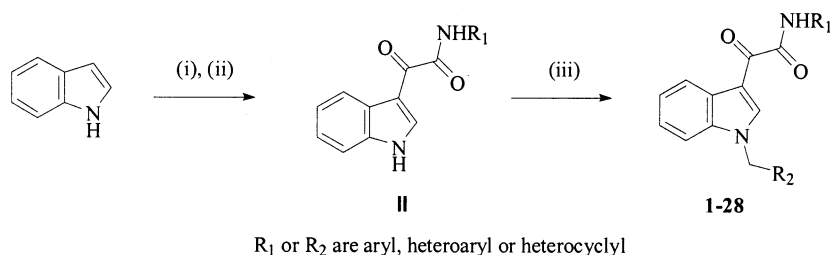
* Author for correspondence. Phone: 886-2-2653-4401 ext. 6587. Fax: 886-2-2792-9703. E-mail: ctchen@nhri.org.tw.

[†] National Health Research Institutes.

[‡] National Yang Ming University.

Scheme 1. Synthesis of Indolyl Glyoxylamides: Route I^a

^a Conditions: (i) *t*BuOK, R₁CH₂X, THF, 0 °C; (ii) oxalyl chloride, Et₂O, 0 °C; (iii) R₂NH₂, Et₃N, THF, 0 °C.

Scheme 2. Synthesis of Indolyl Glyoxylamides: Route II^a

^a Conditions: (i) oxalyl chloride, Et₂O, 0 °C; (ii) R₁NH₂, Et₃N, THF, 0 °C; (iii) *t*BuOK, R₂CH₂X, THF, 0 °C.

substitution reaction with an arylamine. Finally, the *N*-alkylation of indoles was carried out to give the desired *N*-substituted indole glyoxylamides by similar procedures to those described in Route I.

Biology

All of the synthesized indolyl glyoxylamides were screened initially for anticancer activity using the human gastric NUGC3 cells. The selected active indolyl glyoxylamides were then further evaluated to obtain their IC₅₀s, the concentration that causes 50% inhibition of cancer cell growth, against six human cancer cell lines, gastric NUGC3, hepatocellular HepG2, breast MCF7 and its doxorubicin(adriamycin)-resistant MCF7/ADR subline, uterus MES-SA and its doxorubicin-resistant MES-SA/Dx5 subline, and one murine leukemic P388 cell line. Anticancer activity was evaluated with a colorimetric 3-(4,5-dimethylthiazol-2-yl)-5-(3-carboxymethoxyphenyl)-2-(4-sulfophenyl)-2*H*-tetrazolium (MTS) and phenazine methosulfate (PMS) assay system²⁷ by measuring the residual cancer cell activity after treatment with the indolyl glyoxylamides. Apoptotic changes in morphology, nucleus condensation, and apoptotic bodies of the cancer cells upon treatment with indolyl glyoxylamides were visualized with the fluorescent Hoechst staining.²⁸ These compounds also exhibited activity in apoptosis induction as visualized by DNA fragmentation analysis in the human gastric NUGC3 cancer cells. Compounds **7** and **13** with *in vitro* anticancer activities were further evaluated for their *in vivo* anticancer activity with the leukemic P388 cancer survival model in young female inbred DBA/2J mice.²⁹

Results and Discussion

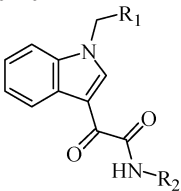
Partition Coefficient. The predicted partition coefficient of indolyl glyoxylamides between water and *n*-octanol was calculated using the fragmental method.³⁰ The AlogP value is an index of the ability of a molecule penetrating the cell membrane and tissue. The predicted AlogP value for D-24851 is 3.30 and those for other

synthesized indolyl glyoxylamides are listed in Table 1. In general, *N*-heterocyclic substitution of indolyl glyoxylamide decreased AlogP and thus increased solubility of the molecules in water. It may be noted, however, that there was no correlation between the AlogP values and the *in vitro* anticancer activity.

In Vitro Anticancer Activity. The IC₅₀ concentration of compounds **1–4**, **6–10**, **13–18**, **20**, **25** and D-24851 were determined and were shown in Table 2. These indolyl glyoxylamides with *N*-heterocyclic rings at R₁- and R₂-positions exhibited a broad spectrum of anticancer activity against the human and murine cancer cells. Most of these compounds were more active than D-24851. Nonetheless, it was noted that D-24851 was comparably more potent against P388 than the other human cancer cells. Selectivity of the activity among these compounds against various human cancer cells was observed. Likewise, these indolyl glyoxylamides with diverse chemical structures also exhibited differential activities in various cancer cell lines. For example, 23 out of 28 compounds were active against NUGC3 cells as shown in Table 1, and 15 out of 17 compounds were relatively active in most of the cell lines tested as indicated in Table 2.

The structures and IC₅₀s in NUGC3 cells of active compounds **11–13**, **21**, **22**, **28** that consist of a five-membered heterocycle and D-24851 that contains a six-membered heterocycle on R₁ were listed in Table 1. The change of a six- to five-membered heterocycle at R₁-position maintains the biological activity. For example, replacement of the aryl chloride of D-24851 with a furyl group of compound **23** at R₁-position showed similar activity against NUGC3 cells. On the other hand, with a five-membered heterocycle on R₂-position, the change from a six- to five-membered heterocycle at R₁-position dramatically increased the activity as noted in compounds **20** and **21**. However, the position of the heteroatom in the heterocycle is extremely important for the R₁-position as indicated by the IC₅₀ of compounds

Table 1. Structure–Activity Relationships of Indolyl Glyoxylamides in Gastric NUGC3 Cells



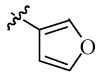
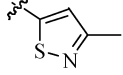
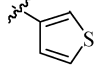
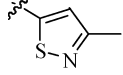
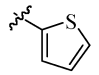
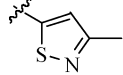
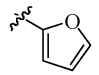
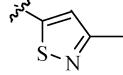
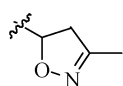
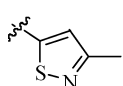
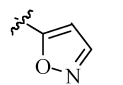
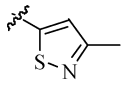
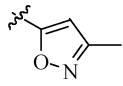
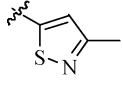
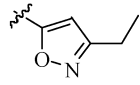
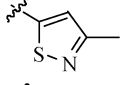
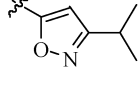
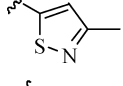
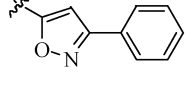
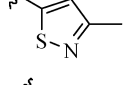
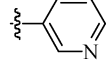
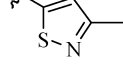
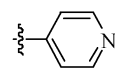
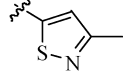
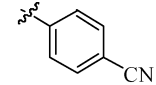
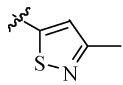
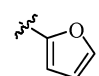
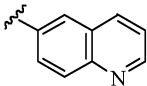
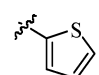
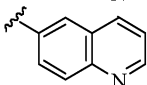
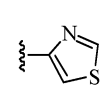
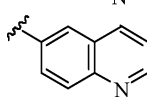
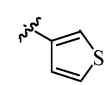
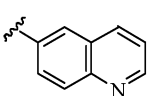
Compound	R ₁	R ₂	m.p. (°C)	AlogP	NUGC3/IC ₅₀ (nM) ^a
1			181-183	2.31	524
2			187-188	2.65	646
3			181-182	2.80	359
4			174-176	2.46	676
5			ND ^b	2.65	>10000
6			211-213	2.01	40
7			244-245	2.18	63
8			277-279	2.80	42
9			298-299	3.37	362
10			204-206	3.86	431
11			192-194	2.27	43
12			246-248	1.92	2913
13			ND ^b	3.61	623
14			160-162	2.83	736
15			196-197	3.17	603
16			192-193	2.52	503
17			203-204	3.02	206

Table 1. (Continued)

Compound	R ₁	R ₂	m.p.(°C)	AlogP	NUGC3/IC ₅₀ (nM) ^a
18			217-214	2.54	262
19			168-169	2.31	3637
20			ND ^b	1.83	478
21			218-220	2.27	>10000
22			ND ^b	3.27	3652
23			167-168	1.66	595
24			221-223	2.11	>10000
25			209-210	1.79	5044
26			178-180	1.77	>10000
27			ND ^b	2.98	>10000
28			ND ^b	3.23	896

^a IC₅₀ values expressed as the mean of triplicate wells of at least three experiments. ^b Not determined because of amorphous solid.

11 and **12**. The isosteric isomer pairs, compounds **1** and **2** or **14** and **15**, showed comparable anticancer activities.

Compounds **7–9** gradually lose their efficacy as the size of alkyl side chain of R₁ (= isoxazolyl) increased. A similar steric hindrance effect was also observed in the case of compounds **25** and **27**. The absence of aromaticity at R₁-position on compound **5** dramatically decreased anticancer activity as compared with the aromatic compound **7**. These observations suggest that the steric and electronic factors may play crucial roles at R₁-position that influences the binding affinity between the compound and its target molecule.

The compounds with a variety of heterocyclic amines at R₂-position were synthesized and evaluated for anticancer activity as listed in Table 1. Replacement of the six-membered pyridine ring of D-24851 with a five-membered heteroaromatic or a bulky quinolyl ring on R₂-position did not significantly change the anticancer activity. As suggested by the data of compounds **2** and **19**, isothiazolylamine appears to be an important moiety at R₂-position. Similar observations were also noted that the potent compounds **6–8** and **11** consist of isothiazolylamine at R₂-position.

The possibility of cross-resistance of these compounds with the other anticancer drugs such as the clinically

frequently used doxorubicin was also explored. Most of these N-heterocyclic indolyl glyoxylamides showed comparative or better efficacy in the two doxorubicin-resistant sublines, breast MCF7/ADR and uterus MES-SA/Dx5 as compared in the parent breast MCF7 and uterus MES-SA cancer cells, indicating no cross-resistance to the multi-drug resistant doxorubicin. The lack of cross-resistance to multiple drugs may be clinically important. On the other hand, compounds **7–9** lose their efficacy gradually with increasing size of alkyl side chain of isoxazolyl R₁. Increasing in the size of the alkyl side chain on R₁, somehow, made these molecules better substrates of the multidrug resistant machinery leading to a gradual loss in activity as suggested by the data in Table 2. In agreement with the previously reported results,⁹ D-24851 showed its efficacy to a similar extent toward both MCF-7 and its multidrug-resistant subline in the present study. The differential IC₅₀ values observed may be due to the utilization of different assay methods (MTS vs 2,3-bis(2-methoxy-4-nitro-5-sulfonyl)-5[(phenylamino)carbonyl]-2H-tetrazolium hydroxide, XTT, or sulforhodamine B, SRB) and treatment periods. The results indicated that the incorporation of heteroatoms at 1- and 3-positions of indolyl glyoxylamide, in general, increases the in vitro anticancer activity.

Table 2. Anticancer Activity of Indolyl Glyoxylamides in Cancer Cell Lines^a

compound	gastric NUGC3	liver HepG2	breast MCF7	breast MCF-7/ADR	uterus MES-SA	uterus MES-SA/DX5	P388
D-24851	524 ± 34	>10000	1134 ± 430	5416 ± 784	7371 ± 164	3018 ± 516	77 ± 15
1	524 ± 26	5962 ± 116	957 ± 18	879 ± 30	652 ± 42	314 ± 17	10 ± 1
2	646 ± 31	2537 ± 162	958 ± 23	338 ± 37	151 ± 5	247 ± 31	167 ± 22
3	359 ± 36	>10000	6825 ± 316	1188 ± 130	729 ± 9	439 ± 36	7 ± 2
4	676 ± 53	7216 ± 723	3592 ± 193	397 ± 24	85 ± 11	26 ± 6	5 ± 1
6	40 ± 6	>10000	2608 ± 135	2333 ± 154	855 ± 205	240 ± 57	6 ± 1
7	63 ± 10	1711 ± 301	73 ± 2	33 ± 7	19 ± 1	17 ± 7	18 ± 2
8	42 ± 5	1149 ± 79	627 ± 77	230 ± 57	32 ± 15	166 ± 37	5 ± 1
9	362 ± 50	>10000	828 ± 72	2131 ± 59	673 ± 11	2132 ± 187	756 ± 138
10	431 ± 81	>10000	946 ± 71	877 ± 46	820 ± 7	512 ± 13	54 ± 27
13	623 ± 126	3663 ± 1970	605 ± 178	619 ± 122	385 ± 54	310 ± 96	12 ± 3
14	736 ± 74	>10000	1260 ± 116	497 ± 12	349 ± 18	279 ± 7	5 ± 4
15	603 ± 23	5668 ± 692	1197 ± 96	961 ± 55	576 ± 8	369 ± 28	62 ± 22
16	503 ± 55	>10000	3085 ± 301	486 ± 39	347 ± 45	280 ± 17	9 ± 1
17	206 ± 10	1889 ± 258	736 ± 115	438 ± 44	378 ± 78	261 ± 27	112 ± 15
18	262 ± 17	1837 ± 61	92 ± 9	95 ± 4	74 ± 20	32 ± 2	3 ± 2
20	478 ± 23	>10000	>10000	>10000	9390 ± 1057	9763 ± 409	>1000
25	5044 ± 103	>10000	>10000	>10000	>10000	>10000	>1000

^a Data were IC₅₀s expressed in nM as mean ± standard deviation of at least three separate experiments.

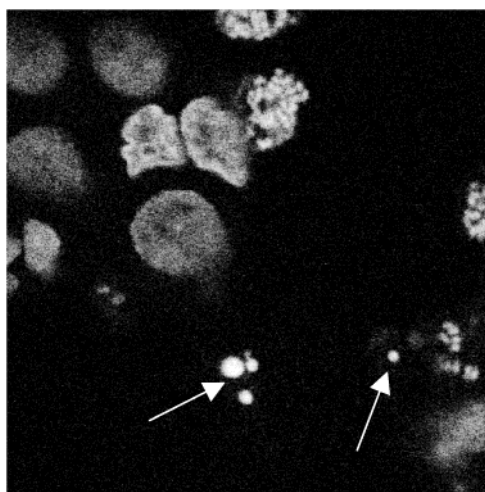


Figure 1. Induction of apoptosis by the treatment with compound **13** at 100 nM for 16 h in human gastric NUGC3 cancer cells. Apoptotic bodies were evident by Hoechst 33258 staining as indicated in arrows.

Apoptosis Induction. Human gastric NUGC3 cancer cells were treated with indolyl glyoxylamides for 16 h, and the apoptosis induction was observed by the morphological change in nucleus condensation, formation of apoptotic bodies, and as demonstrated by DNA fragmentation analysis. As shown in Figure 1, apoptotic bodies of the cancer cells treated with compound **13** at 100 nM were observed after Hoechst staining with a fluorescent microscope. As shown in Figure 2, several indolyl glyoxylamides at 100 nM induced DNA fragmentation after a 24-h treatment in the cancer cells. The findings indicate that apoptosis induction may be a mechanism by which these *N*-heterocyclic indolyl glyoxylamides kill the cancer cells. The molecular target(s) of these new indolyl glyoxylamides is under investigation although the anticancer activity of D-24851 can be explained by an interaction with the tubulin.⁹

In Vivo Activity of Prolongation in Cancer Survival. Female DBA/2J mice of a negative, vehicle control group consistently survived for 7 to 8 days after a single intravenous inoculation of one million murine leukemic P388 cancer cells. In the control experiment, doxorubicin showed a consistent activity in prolongation

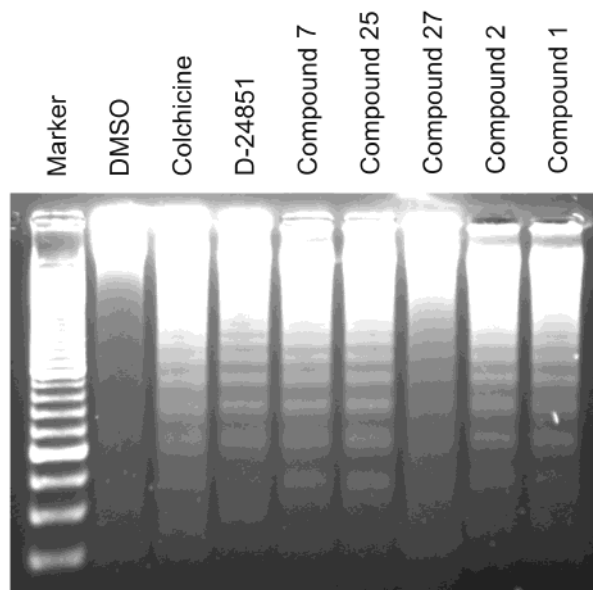


Figure 2. DNA fragmentation was observed in human gastric NUGC3 cancer cells treated with several *N*-heterocyclic indolyl glyoxylamides.

of the survival period in the P388-inoculated DBA/2J mice. The increase of life span by treatment with doxorubicin at its maximal tolerated dose was 119 ± 18% (mean ± standard deviation) and was used as an experimental quality control for each experiment. Compounds **7** and **13** exhibited dose-dependent activities in increasing the life span of cancer-bearing animals as shown in Figure 3. The *in vivo* dose-response relationship ($p < 0.05$, ANOVA) of **7**, **13** and D-24851 in prolonging cancer survival in animals was summarized in Table 3. An oral dose-dependent *in vivo* activity between **7** and D-24851 was observed. Compound **7** and D-24851 showed equal activity in the prolongation of cancer survival at oral doses up to 100 mg/kg, whereas D-24851 was more active at the highest given oral dose, 200 mg/kg. Further prolongation of cancer survival was observed after a continuation of up to 9 days of daily oral administrations with **7** and **13** without evident loss of body weight (data not shown).

As shown in Table 2, the *in vitro* potency of **7** and **13** was approximately 4- and 6-fold, respectively, higher

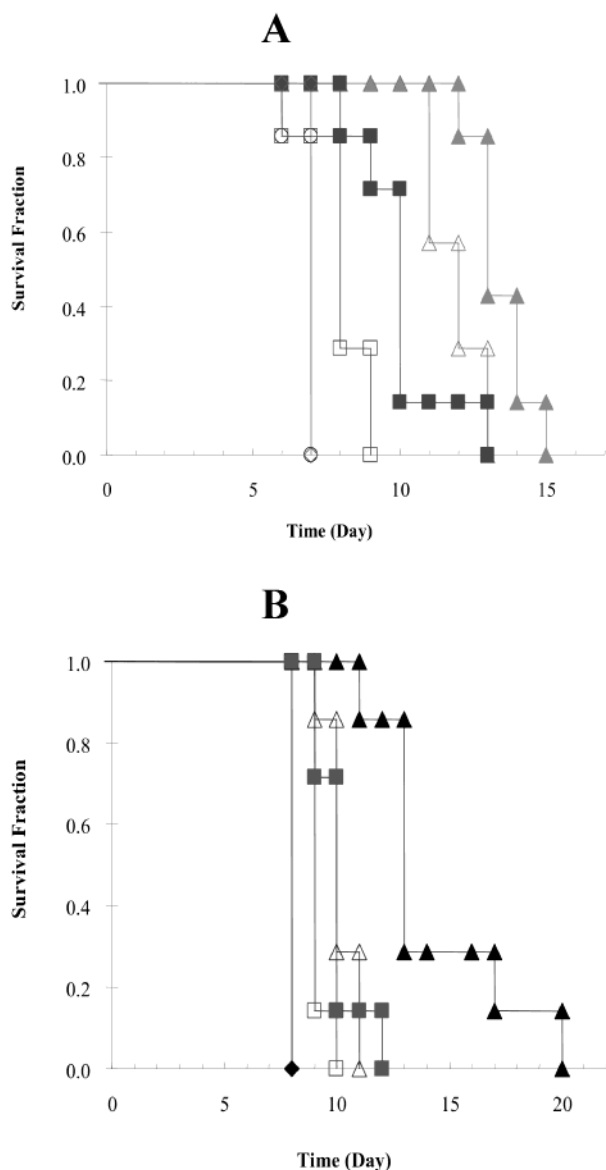


Figure 3. Prolongation of cancer survival in leukemic DBA/2J mice orally gavaged with compounds **7** (A) and **13** (B). A dose-response relationship was observed. A. \diamond : 5, \square : 25, \blacksquare : 50, \triangle : 100, \blacktriangle : 200 mg/kg compound **7**, \circ : 0.5% CMC vehicle control; B. \square : 25, \blacksquare : 50, \triangle : 100, \blacktriangle : 200 mg/kg compound **13**, \blacklozenge : 0.5% CMC vehicle control.

than that of D-24851 against the growth of P388 cells. D-24851, however, showed equal or better in vivo oral activity compared to **7** and **13** in prolonging the survival of P388-inoculated animals. The oral dose-dependent difference in in vivo activity between **7** and D-24851 implies a possible involvement of the pharmacokinetic processes, absorption, distribution, metabolism, and excretion. Pharmacokinetic characteristics usually accounts for uncorrelated activities between in vitro and in vivo results. For example, intestinal P-glycoprotein limits oral bioavailability of paclitaxel and thus its oral uses.³¹ Promising P-glycoprotein inhibitors have been developed to increase the oral bioavailability of drugs.^{32,33} These observations warrant further detailed pharmacokinetic studies for the *N*-heterocyclic indolyl glyoxylamides. Nonetheless, results of the leukemic P388 cancer survival model showed that the *N*-heterocyclic substitution retains the in vivo anticancer activity and

Table 3. Prolongation of Cancer Survival in P388-Inoculated Leukemic Mice by Treatments of **7**, **13**, and D-24851

dose, mg/kg ^a	7 , %	13 , %	D-24851, %
25	26 ± 27 ^b	14 ± 1	27 ± 9
50	57 ± 20	27 ± 3	44 ± 22
100	63 ± 17 ^c	20 ± 8 ^c	63 ± 14 ^c
200	100 ± 21 ^d	46 ± 24 ^d	149 ± 28 ^d

^a The doses were administered daily on the next day after P388-inoculation for 4 days. ^b The data in mean ± standard deviation of three separate experiments were expressed as the percentage of increase in life span compared in medium survival time. Medium survival time is the time when 50% of the P388-inoculated mice in a dosing group are still surviving. ^c $p < 0.05$ (ANOVA) for both **7** vs **13** and **13** vs D-24851. ^d $p < 0.05$ (ANOVA) for **7** vs **13**, **7** vs D-24851, and **13** vs D-24851.

further demonstrated an oral anticancer activity of these *N*-heterocyclic indolyl glyoxylamides.

It was noted that D-24851 was selectively more potent against murine P388 than the human tumor cells. The difference between the IC₅₀ of the human tumor cells and that of murine P388 cells for the analogues was generally less than that for D-24851, implying a possible oral activity for compound **7** against in vivo growth of the human tumor cells. While orally active against the leukemic cancer, this observation encourages exploration on the oral activity spectrum against the growth of human solid tumor xenografts in animals and further development.

Conclusion

Cancer is the leading cause of death in the developed countries. Although chemotherapy is one of the major treatment options available for cancer, the mechanism of action of some effective anticancer drugs remains unclear. Most of the currently used anticancer drugs are chemicals of small molecule and administered into patients via a parenteral infusion or bolus injection. Clinical complications with the parenteral administrations have been documented, and thus extra cares and cost associated with hospitalization are necessary. Recent efforts in the discovery of anticancer drugs have been focused on searching for orally active anticancer agents. *N*-Heterocyclic indolyl glyoxylamides induce apoptosis in cancer cells and demonstrate oral activity against cancer in animals and may be further explored as anticancer therapeutics.

Experimental Section

In Vitro Growth Inhibition Study. A murine leukemic P388 cell line and a panel of human cancer cell lines, gastric NUGC3, hepatocellular HepG2, breast MCF7 and its doxorubicin-resistant MCF7/ADR subline, uterus MES-SA and its doxorubicin-resistant MES-SA/Dx5 subline purchased from the Food Industry Research and Development Institute (Hsinchu, Taiwan), Japanese Collection of Research Bioresources, National Institute of Health Sciences (Tokyo, Japan) and from American Type Culture Collection (Manassas, VA), were seeded at a cell density of 3000 or 4500 for human cancer and 10000 for murine cancer cells/100 μ L/well, respectively, in 96-well flat-bottom plates and incubated for 24 h at 37 °C in a 5% CO₂ incubator. Testing compounds were dissolved in dimethyl sulfoxide (DMSO) purchased from Sigma (St. Louis, MO) and further diluted into the culture medium for treatments of human cancer cells. The testing sample-containing media had a final DMSO concentration of $\leq 0.3\%$ for in vitro testing at various concentrations. Culture media with 10 nM actinomycin D and 0.3% DMSO were used as the positive reference and vehicle control, respectively. Cancer cells were

treated in duplicate wells per concentration (200 μ L/well) for 72 h at 37 °C, 5% CO₂ in an incubator. A colorimetric assay using MTS/PMS system was used to determine the anticancer activity of the testing compounds.²⁷ Both MTS and PMS were purchased from Promega Corp. (Madison, WI). The colorimetric assay measures cell viability based on the cellular activity in conversion of a tetrazolium salt into a colored soluble formazan product. The optical density (OD) values were measured at 490 nm with a 1420 multilabel counter VICTOR from Wallac (Turku, Finland). The IC₅₀ of an *N*-heterocyclic indolyl glyoxylamide that inhibits 50% of the growth activity of cancer cells was then determined.

Hoechst 33258 Staining. Gastric NUGC3 cancer cells of 5×10^5 seeded in a six-well culture plate were allowed to attach for 24 h. Cells were then treated with compounds of various concentrations at 37 °C in a CO₂ incubator for another 16 h. The cells were washed with PBS and fixed with 2% formalin at room temperature for 10 min. After being rinsed with PBS, the cells were incubated in the staining solution (1 μ g/mL Hoechst 33258 and 0.1% Triton X-100 in PBS) at room temperature for 5 min followed by washing with PBS and examination with a fluorescent microscope.

DNA Fragmentation Analysis. Oligonucleosomal fragments of the genomic DNA induced by treatment with the indolyl glyoxylamides in gastric NUGC3 cancer cells were isolated and assessed by agarose gel electrophoresis as previously described procedures with modification.²⁸ In brief, 2×10^6 cancer cells were incubated with an appropriate compound for an optimal period of time and concentration. Both floating and adherent cells were collected at the end of incubation, washed once with PBS, and resuspended in the lysis buffer. After incubation at 50 °C overnight, the samples were treated with RNase A at 37 °C for 1 h. The DNA was extracted with a mixture of phenol:chloroform:isoamyl alcohol (25:24:1), and the supernatant was collected, separated on a 2% agarose gel, and stained with ethidium bromide. Colchicine was used as a positive control.

In Vivo Cancer Survival Study. The in vivo anticancer activity of the compounds was evaluated by the murine leukemic P388 model.²⁹ Inbred five-week old female DBA/2J mice were purchased from the National Laboratory Animals Breeding and Research Center (Taipei, Taiwan). Murine leukemic P388 cells were purchased from the Japanese Collection of Research Bioresources, Japan. P388 cells were cultured and propagated in RPMI1640 medium supplemented with the MEM-nonessential amino acids, 50 μ M 2-mercaptoethanol, and 10% fetal bovine serum. Mice were grouped as the treatment, negative control and positive control groups at 7 to 8 mice per treatment group. All mice were intravenously inoculated with one million P388 cells per mouse 1 day before the treatments initiated. Compounds were dissolved in DMSO and then diluted with 0.5% carboxymethyl cellulose with the final concentration of DMSO less than 0.5%. The compounds were orally gavaged (po) to the mice (0.1 mL per mouse) at various doses to show a pharmacological dose-response relationship. Mice of the negative control group were treated only with the dosing vehicle, 0.5% carboxymethyl cellulose. Doxorubicin of maximal tolerated dose (10 mg/kg, iv) was used as a positive experimental reference. The cancer cell-inoculated animals were monitored twice daily. Survival fractions of the mice were recorded for each treatment group. A time period that 50% of the P388-inoculated mice still survive is defined as the medium survival time and used to calculate a percentage (normalized to the medium survival time of the control group) of increase in life span after treatments. The percentage of increase in life span is then used as an index for treatment response. The study was performed three times to obtain the percentage expressed in mean \pm standard deviation for each dosing group.

Synthesis. All commercially available materials were used without further purification unless otherwise stated. Tetrahydrofuran and diethyl ether were distilled from sodium benzophenone ketyl. CH₂Cl₂ was distilled from P₂O₅. Triethylamine was dried over KOH and distilled. Solvents used for

spectral measurements were of spectrograde. Preparative separations were performed with flash column chromatography (Merck silica gel 60, particle size 230–400 mesh) and analytical TLC was performed on precoated plates (Merck silica gel 60 F₂₅₄); compounds were visualized by using UV light, I₂ vapor, or 2.5% phosphomolybdic acid in ethanol with heating.

Melting points were measured with a Yanaco (MP-500D) melting point apparatus. Predicted AlogP³⁰ values were calculated using the Cerius^{II} interface from Accelrys Inc. (San Diego, CA). Infrared (IR) spectra were recorded on a Perkin-Elmer (Spectrum RX1) spectrophotometer. The proton NMR spectra were obtained on a Varian Mer-Vx-300 (300 MHz) Spectrometer. Chloroform-*d* and dimethyl sulfoxide-*d*₆ were used as solvent; Me₄Si (δ 0.00) was used as an internal standard. All NMR chemical shifts are reported as δ values, and coupling constants (*J*) are given in hertz (Hz). The splitting pattern abbreviations are as follows; s, singlet; d, doublet; t, triplet; q, quartet; br, broad; m, unresolved multiplet and dd, doublet of doublet. Mass spectra were carried out on a Hewlett-Packard (1100 MSD) mass spectrometer. Microanalyses were performed on a Heraeus CHN–O Rapid microanalyzer at the NCTU Instrument Center at National Chiao Tung University, Hsinchu, Taiwan.

General Procedure for the Synthesis of 1–4, 11–12, 14, 16–17, 19, 21, 23. **N₁-(3-Methyl-5-isothiazolyl)-2-[1-(2-furylmethyl)-1*H*-3-indolyl]-2-oxoacetamide (1).** To a mixture of indole (1.17 g, 10 mmol) in tetrahydrofuran (10 mL) was added a solution of potassium *tert*-butoxide (1.34 g, 12 mmol) in tetrahydrofuran (10 mL) at 0 °C and stirred at room temperature for 1 h. 3-(Bromomethyl)furan (1.61 g, 10 mmol) was added, and the mixture was stirred at room temperature for 4 h. After the reaction was quenched with the addition of saturated aqueous NH₄Cl solution, the mixture was extracted with several portions of EtOAc. The combined EtOAc solution was dried with MgSO₄ and concentrated in vacuo. The residue was purified by silica gel column chromatography (EtOAc/hexane = 1:4) to give 1-(3-furylmethyl)-1*H*-indole (1.73 g, 88%) as a yellow solid.

To a solution of 1-(3-furylmethyl)-1*H*-indole (197 mg, 1.0 mmol) in diethyl ether (10 mL) was added oxalyl chloride (254 mg, 2.0 mmol) dropwise at 0 °C. The reaction mixture was stirred at 0 °C for 3 h, and the solvent was removed under reduced pressure. The residue was dissolved in tetrahydrofuran (5 mL) and 5-amino-3-methylisothiazole hydrochloride (151 mg, 1.0 mmol) was added. The mixture was stirred for 3 h and quenched with a saturated aqueous NaHCO₃ solution (4 mL). The organic layer was separated and washed with brine (20 mL). The aqueous layer was extracted with ethyl acetate (20 mL \times 3). The combined organic layer was dried with MgSO₄ and concentrated in vacuo. The crude mixture was purified by silica gel column chromatography (EtOAc/hexane = 1: 2) to give **1** as a yellow solid (259 mg, 71%). ¹H NMR (CDCl₃): δ 10.35 (s, 1H), 9.10 (s, 1H), 8.45 (dd, *J* = 6.2, 1.8 Hz, 1H), 7.46–7.36 (m, 5H), 6.8 (s, 1H), 6.32 (d, *J* = 1.2 Hz, 1H), 5.26 (s, 2H), 2.46 (s, 3H). ESMS *m/z* 366.0 (MH⁺).

N₁-(3-Methyl-5-isothiazolyl)-2-oxo-2-[1-(3-thienylmethyl)-1*H*-3-indolyl]acetamide (2). Yield: 68%. Yellow solid. ¹H NMR (CDCl₃): δ 10.42 (s, 1H), 9.05 (s, 1H), 8.37 (d, *J* = 7.5 Hz, 1H), 7.31–7.19 (m, 4H), 7.07 (s, 1H), 6.89 (d, *J* = 4.8 Hz, 1H), 6.73 (s, 1H), 5.33 (s, 2H), 2.36 (s, 3H). ESMS *m/z* 382.1 (MH⁺).

N₁-(3-Methyl-5-isothiazolyl)-2-oxo-2-[1-(2-thienylmethyl)-1*H*-3-indolyl]acetamide (3). Yield: 65%. Yellow solid. ¹H NMR (CDCl₃): δ 10.37 (s, 1H), 9.14 (s, 1H), 8.46–8.43 (m, 1H), 7.46–7.26 (m, 5H), 6.92 (d, *J* = 3.6 Hz, 1H), 6.81 (s, 1H), 5.47 (s, 2H), 2.46 (s, 3H). ESMS *m/z* 382.0 (MH⁺).

N₁-(3-Methyl-5-isothiazolyl)-2-[1-(2-furyl)-1*H*-3-indolyl]-2-oxoacetamide (4). Yield: 69%. Brown solid. ¹H NMR (CDCl₃): δ 10.36 (s, 1H), 9.13 (s, 1H), 8.45–8.42 (m, 1H), 7.55–7.52 (m, 1H), 7.42–7.37 (m, 3H), 6.80 (s, 1H), 6.42–6.34 (m, 2H), 5.36 (s, 2H), 2.46 (s, 3H). ESMS *m/z* 366.3 (MH⁺).

N₁-(3-Methyl-5-isothiazolyl)-2-[1-(3-methyl-4,5-dihydro-5-isoxazolyl)methyl]-1*H*-3-indolyl-2-oxoacetamide (5).

Yield: 68%. Yellow solid. $^1\text{H NMR}$ (CDCl_3): δ 10.44 (s, 1H), 9.03 (s, 1H), 8.36 (d, $J = 7.2$ Hz, 1H), 7.46 (d, $J = 4.5$ Hz, 1H), 7.35–7.28 (m, 3H), 5.08–5.02 (m, 1H), 4.35–4.30 (m, 2H), 3.14 (dd, $J = 17.0$, 10.5 Hz, 1H), 2.78 (dd, $J = 17.0$, 6.9 Hz, 1H), 2.45 (s, 3H), 2.00 (s, 3H). ESMS m/z 383.1 (MH^+). Anal. ($\text{C}_{19}\text{H}_{18}\text{N}_4\text{O}_3\text{S}$) C, H, N.

N_1 -(3-Methyl-5-isothiazolyl)-2-[1-(5-isoxazolylmethyl)-1H-3-indolyl]-2-oxoacetamide (6). Yield: 72%. Yellow solid. $^1\text{H NMR}$ (CDCl_3): δ 12.76 (s, 1H), 9.12 (s, 1H), 8.52 (d, $J = 1.5$ Hz, 1H), 8.32–8.29 (m, 1H), 7.73–7.69 (m, 1H), 7.38–7.35 (m, 2H), 7.05 (s, 1H), 6.56 (d, $J = 1.5$ Hz, 1H), 5.91 (s, 2H), 2.34 (s, 3H). ESMS m/z 367.0 (MH^+). Anal. ($\text{C}_{18}\text{H}_{14}\text{N}_4\text{O}_3\text{S}$) C, H, N.

N_1 -(3-Methyl-5-isothiazolyl)-2-1-[(3-methyl-5-isoxazolyl)methyl]-1H-3-indolyl-2-oxoacetamide (7). Yield: 77%. Yellow solid. $^1\text{H NMR}$ (CDCl_3): δ 10.33 (s, 1H), 9.15 (s, 1H), 8.44 (d, $J = 6.3$ Hz, 1H), 7.45–7.38 (m, 3H), 6.82 (s, 1H), 5.96 (s, 1H), 5.48 (s, 2H), 2.49 (s, 3H), 2.52 (s, 3H). HRMS calcd for $\text{C}_{19}\text{H}_{16}\text{N}_4\text{O}_3\text{S}$ 380.0943, found 380.0940. Anal. ($\text{C}_{19}\text{H}_{16}\text{N}_4\text{O}_3\text{S}$) C, H, N.

N_1 -(3-Methyl-5-isothiazolyl)-2-1-[(3-ethyl-5-isoxazolyl)methyl]-1H-3-indolyl-2-oxoacetamide (8). Yield: 68%. Yellow solid. $^1\text{H NMR}$ (CDCl_3): δ 10.26 (bs, 1H), 9.14 (s, 1H), 8.68–8.41 (m, 1H), 7.43–7.39 (m, 3H), 6.79 (s, 1H), 5.95 (s, 1H), 5.46 (s, 2H), 2.62 (q, $J = 7.5$ Hz, 2H), 2.46 (s, 3H), 1.20 (t, $J = 7.5$ Hz). HRMS calcd for $\text{C}_{20}\text{H}_{18}\text{N}_4\text{O}_3\text{S}$ 394.1100, found 394.1104.

N_1 -(3-Methyl-5-isothiazolyl)-2-1-[(3-isopropyl-5-isoxazolyl)methyl]-1H-3-indolyl-2-oxoacetamide (9). Yield: 67%. Yellow solid. $^1\text{H NMR}$ (CDCl_3): δ 10.32 (s, 1H), 9.16 (s, 1H), 8.46–8.43 (m, 1H), 7.48–7.37 (m, 3H), 6.81 (s, 1H), 5.98 (s, 1H), 5.47 (s, 2H), 3.07–2.93 (m, 1H), 2.47 (s, 3H), 1.24 (t, $J = 5.1$ Hz, 6H). ESMS m/z 409.1 (MH^+).

N_1 -(3-Methyl-5-isothiazolyl)-2-oxo-2-1-[(3-phenyl-5-isoxazolyl)methyl]-1H-3-indolylacetamide (10). Yield: 63%. Yellow solid. $^1\text{H NMR}$ (CDCl_3): δ 10.29 (s, 1H), 9.21 (s, 1H), 8.46 (dd, $J = 5.4$, 2.7 Hz, 1H), 7.72 (dd, $J = 6.8$, 2.4 Hz, 2H), 7.50–7.37 (m, 6H), 6.81 (s, 1H), 6.42 (s, 1H), 5.56 (s, 2H), 2.47 (s, 3H). ESMS m/z 443.1 (MH^+).

N_1 -(3-Methyl-5-isothiazolyl)-2-oxo-2-1-[(3-pyridylmethyl)-1H-3-indolyl]acetamide (11). Yield: 67%. Yellow solid. $^1\text{H NMR}$ ($\text{DMSO}-d_6$): δ 12.75 (s, 1H), 9.20 (s, 1H), 8.66 (d, $J = 1.5$ Hz, 1H), 8.49 (dd, $J = 4.8$, 1.5 Hz, 1H), 8.31 (dd, $J = 5.4$, 2.7 Hz, 1H), 7.73–7.66 (m, 2H), 7.37–7.31 (m, 3H), 7.05 (s, 1H), 5.70 (s, 2H), 2.35 (s, 3H). ESMS m/z 377.0 (MH^+).

N_1 -(3-Methyl-5-isoxazolyl)-2-oxo-2-1-[(4-pyridylmethyl)-1H-3-indolyl]acetamide (12). Yield: 73%. Yellow solid. $^1\text{H NMR}$ (CDCl_3): δ 10.10 (s, 1H), 9.05 (s, 1H), 8.60 (d, $J = 5.1$ Hz, 2H), 8.48 (d, $J = 7.8$ Hz, 1H), 7.44–7.22 (m, 3H), 7.05 (d, $J = 5.1$ Hz, 2H), 6.35 (s, 1H), 5.45 (s, 2H), 2.32 (s, 3H). HRMS calcd for $\text{C}_{20}\text{H}_{16}\text{N}_4\text{O}_3$ 360.1222, found 360.1228.

N_1 -(3-Methyl-5-isothiazolyl)-2-1-(4-cyanobenzyl)-1H-3-indolyl-2-oxoacetamide (13). Yield: 71%. Yellow solid. $^1\text{H NMR}$ (CDCl_3): δ 9.39 (s, 1H), 9.15 (s, 1H), 8.46 (d, $J = 9.0$ Hz, 1H), 7.65–7.21 (m, 11H), 5.48 (s, 2H). ESMS m/z 401.2 (MH^+).

N_1 -(6-Quinolyl)-2-1-(2-furylmethyl)-1H-3-indolyl-2-oxoacetamide (14). Yield: 84%. Yellow solid. $^1\text{H NMR}$ (CDCl_3): δ 9.56 (s, 1H), 9.10 (s, 1H), 8.81 (d, $J = 3.9$ Hz, 1H), 8.45–8.40 (m, 2H), 8.12 (d, $J = 8.7$ Hz, 1H), 8.06 (d, $J = 8.7$ Hz, 1H), 7.73 (dd, $J = 9.0$, 2.4 Hz, 1H), 7.48–7.31 (m, 4H), 7.19 (s, 1H), 6.35–6.29 (m, 2H), 5.30 (s, 2H). HRMS calcd for $\text{C}_{24}\text{H}_{17}\text{N}_3\text{O}_3$ 395.1270, found 395.1270. Anal. ($\text{C}_{24}\text{H}_{17}\text{N}_3\text{O}_3$) C, H, N.

N_1 -(6-Quinolyl)-2-oxo-2-1-(2-thienylmethyl)-1H-3-indolylacetamide (15). Yield: 81%. Yellow solid. $^1\text{H NMR}$ (CDCl_3): δ 9.64 (s, 1H), 9.18 (s, 1H), 8.88 (dd, $J = 4.2$, 1.8 Hz, 1H), 8.51–8.48 (m, 2H), 8.16 (dd, $J = 9.0$, 0.9 Hz, 1H), 8.12 (d, $J = 9.0$ Hz, 1H), 7.79 (dd, $J = 9.0$, 2.4 Hz, 1H), 7.49–7.36 (m, 4H), 7.29–7.26 (m, 1H), 7.07 (dd, $J = 3.6$, 1.2 Hz, 1H), 6.98 (dd, $J = 5.1$, 3.6 Hz, 1H), 5.56 (s, 2H). ESMS m/z 412.0 (MH^+).

N_1 -(5-Quinolyl)-2-1-(4-isothiazolylmethyl)-1H-3-indolyl-2-oxoacetamide (16). Yield: 81%. Yellow solid. $^1\text{H NMR}$ (CDCl_3): δ 9.64 (s, 1H), 9.25 (s, 1H), 8.87 (dd, $J = 4.2$, 1.8 Hz,

1H), 8.83 (d, $J = 2.1$ Hz, 1H), 8.52–8.48 (m, 2H), 8.19–8.11 (m, 2H), 7.80 (dd, $J = 9.0$, 2.4 Hz, 1H), 7.48–7.33 (m, 4H), 7.08 (d, $J = 2.1$ Hz, 1H), 5.61 (s, 2H). ESMS m/z 413.1 (MH^+).

N_1 -(6-Quinolyl)-2-oxo-2-1-(3-thienylmethyl)-1H-3-indolylacetamide (17). Yield: 78%. Yellow solid. $^1\text{H NMR}$ (CDCl_3): δ 9.66 (s, 1H), 9.17 (s, 1H), 8.88 (dd, $J = 4.2$, 1.8 Hz, 1H), 8.51–8.48 (m, 2H), 8.15 (dd, $J = 13.8$, 7.5 Hz, 2H), 7.79 (dd, $J = 9.0$, 2.4 Hz, 1H), 7.44–7.32 (m, 5H), 7.16 (d, $J = 1.8$ Hz, 1H), 6.99 (dd, $J = 4.8$, 1.2 Hz, 1H), 5.42 (s, 2H). HRMS calcd for $\text{C}_{24}\text{H}_{17}\text{N}_3\text{O}_3\text{S}$ 411.1041, found 411.1033. Anal. ($\text{C}_{24}\text{H}_{17}\text{N}_3\text{O}_3\text{S}$) C, H, N.

General Procedure for the Synthesis of 5–10, 18, 20, 25. **N_1 -(6-Quinolyl)-2-1-[(3-methyl-5-isoxazolyl)methyl]-1H-3-indolyl-2-oxoacetamide (18)**. To a mixture of propargyl chloride (2.79 g, 37.5 mmol), acetaldoxime (2.23 g, 37.4 mmol), and triethylamine (2 mL) in CH_2Cl_2 (100 mL) was added sodium hypochlorite (67.1 mL, 13% active chlorine) at 0 °C. The reaction mixture was allowed to warm to room temperature, and stirring was continued at room temperature for 3 h. The mixture was quenched with water, and the aqueous solution was extracted with CH_2Cl_2 and dried over Na_2SO_4 . After removal of the solvent, the residue was chromatographed on silica gel (EtOAc/hexane = 1:4) to give 5-(chloromethyl)-3-methylisoxazole (4.5 g, 46%) as a colorless liquid.

To a mixture of indole (1.17 g, 10 mmol) in tetrahydrofuran (10 mL) was added a solution of potassium *tert*-butoxide (1.34 g, 12 mmol) in tetrahydrofuran (10 mL) at 0 °C, and the mixture was stirred at 0 °C for 30 min. This was followed by the addition of 5-(chloromethyl)-3-methylisoxazole (1.32 g, 10 mmol) and stirring at room temperature for 4 h. The reaction was quenched at room temperature with a saturated aqueous NH_4Cl solution and extracted with several portions of CH_2Cl_2 . The combined organic layer was dried with MgSO_4 and concentrated. The crude product was purified by silica gel flash column chromatography (EtOAc/hexane = 1:4) to give 5-(1H-1-indolylmethyl)-3-methylisoxazole (1.61 g, 76%) as a yellow solid.

To a solution of 5-(1H-1-indolylmethyl)-3-methylisoxazole (232 mg, 1.0 mmol) in diethyl ether (10 mL) was added oxalyl chloride (254 mg, 2.0 mmol) dropwise at 0 °C. The reaction mixture was stirred at 0 °C for 3 h, and the solvent was concentrated in vacuo to remove the diethyl ether and then dissolved in tetrahydrofuran (5 mL). To the mixture were added 6-quinolylamine (216 mg, 1.5 mmol) and triethylamine (5 mL), and the mixture was stirred for 3 h at room temperature. A saturated aqueous NaHCO_3 solution (4 mL) was added to quench the reaction and the reaction mixture extracted with ethyl acetate. The combined extracts were dried with MgSO_4 and concentrated in vacuo. The crude compound was purified by column chromatography (EtOAc/hexane = 1:1) to give **10** as a yellow solid (303 mg, 74%). $^1\text{H NMR}$ (CDCl_3): δ 9.61 (s, 1H), 9.20 (s, 1H), 8.88 (dd, $J = 4.2$, 1.5 Hz, 1H), 8.50 (dd, $J = 9.5$, 1.5 Hz, 2H), 8.16 (dd, $J = 14.0$, 9.5 Hz, 2H), 7.80 (dd, $J = 3.3$, 2.4 Hz, 1H), 7.45–7.38 (m, 4H), 5.95 (s, 1H), 5.48 (s, 2H), 2.25 (s, 3H). ESMS m/z 411.2 (MH^+).

N_1 -(3-Methyl-5-isoxazolyl)-2-oxo-2-1-(3-thienylmethyl)-1H-3-indolylacetamide (19). Yield: 74%. Yellow solid. $^1\text{H NMR}$ (CDCl_3): δ 10.07 (s, 1H), 9.00 (s, 1H), 8.47–8.43 (m, 1H), 7.43–7.31 (m, 4H), 7.15 (dd, $J = 2.9$, 1.2 Hz, 1H), 6.97 (dd, $J = 5.0$, 1.2 Hz, 1H), 6.35 (s, 1H), 5.41 (s, 2H), 2.32 (s, 3H). HRMS calcd for $\text{C}_{19}\text{H}_{15}\text{N}_3\text{O}_3\text{S}$ 365.0834, found 365.0829. Anal. ($\text{C}_{19}\text{H}_{15}\text{N}_3\text{O}_3\text{S}$) C, H, N.

N_1 -(3-Methyl-5-isothiazolyl)-2-1-[(3-methyl-5-isoxazolyl)methyl]-1H-3-indolyl-2-oxoacetamide (20). Yield: 71%. Yellow solid. $^1\text{H NMR}$ (CDCl_3): δ 10.03 (s, 1H), 9.05 (s, 1H), 8.47–8.44 (m, 1H), 7.46–7.38 (m, 3H), 6.37 (s, 1H), 5.95 (s, 1H), 5.48 (s, 2H), 2.33 (s, 3H), 2.54 (s, 3H). ESMS m/z 364.4 (MH^+).

N_1 -(3-Methyl-5-isothiazolyl)-2-oxo-2-1-(4-pyridylmethyl)-1H-3-indolylacetamide (21). Yield: 69%. Yellow solid. $^1\text{H NMR}$ (CDCl_3): δ 10.34 (s, 1H), 9.18 (s, 1H), 8.60 (d, $J = 6.0$ Hz, 2H), 8.48 (d, $J = 7.8$ Hz, 1H), 7.45–7.22 (m, 4H), 7.08

(d, $J = 6.0$ Hz, 2H), 6.82 (s, 1H), 5.47 (s, 2H), 2.47 (s, 3H). ESMS m/z 377.1 (MH⁺). Anal. (C₂₀H₁₆N₄O₂S) C, H, N.

N₁-(3-Methyl-5-isoxazolyl)-2-[1-(4-cyanobenzyl)-1H-3-indolyl]-2-oxoacetamide (22). Yield: 69%. Yellow solid. ¹H NMR (CDCl₃): δ 10.07 (s, 1H), 9.04 (s, 1H), 8.48 (d, $J = 8.1$ Hz, 1H), 7.65 (d, $J = 8.4$ Hz, 2H), 7.44–7.22 (m, 5H), 6.35 (s, 1H), 5.50 (s, 2H), 2.33 (s, 3H). ESMS m/z 385.0 (MH⁺).

N₁-(4-Pyridyl)-2-[1-(2-furylmethyl)-1H-3-indolyl]-2-oxoacetamide (23). Yield: 74%. Yellow solid. ¹H NMR (CDCl₃): δ 9.44 (s, 1H), 9.00 (s, 1H), 8.46 (dd, $J = 4.7, 1.5$ Hz, 2H), 8.39–8.36 (m, 1H), 7.58 (dd, $J = 4.8, 1.5$ Hz, 2H), 7.47–7.28 (m, 4H), 6.35–6.28 (m, 2H), 5.29 (s, 2H). HRMS calcd for C₂₀H₁₅N₃O₃ 345.1113, found 345.1115.

N₁-(5-Methyl-3-isoxazolyl)-2-[1-(1-methyl-1H-5-imidazolyl)methyl]-1H-3-indolyl-2-oxoacetamide (24). Yield: 59%. Yellow solid. ¹H NMR (CDCl₃): δ 11.46 (br, 1H), 8.78 (s, 1H), 8.25–8.22 (m, 1H), 7.71–7.69 (m, 1H), 7.32–7.29 (m, 2H), 7.12 (s, 1H), 6.83 (s, 1H), 6.69 (s, 1H), 5.55 (s, 2H), 3.69 (s, 3H), 2.41 (s, 3H). HRMS calcd for C₁₉H₁₇N₅O₃ 363.1331, found 363.1347.

N₁-(4-Methyl-1,3-thiazol-2-yl)-2-[1-(3-methyl-5-isoxazolyl)methyl]-1H-3-indolyl-2-oxoacetamide (25). Yield: 73%. Yellow solid. ¹H NMR (CDCl₃): δ 9.10 (s, 1H), 8.46–8.43 (m, 1H), 7.41–7.34 (m, 4H), 6.63 (s, 1H), 5.90 (s, 1H), 5.43 (s, 2H), 2.34 (s, 3H), 2.21 (s, 3H). ESMS m/z 381.0 (MH⁺).

N₁-(4-Methyl-1,3-thiazol-2-yl)-2-[1-(4-thiazolylmethyl)-1H-3-indolyl]-2-oxoacetamide (26). Yield: 81%. Yellow solid. ¹H NMR (CDCl₃): δ 9.19 (s, 1H), 8.55 (d, $J = 2.1$ Hz, 1H), 8.49–8.46 (m, 1H), 7.46–7.31 (m, 4H), 7.06 (s, 1H), 6.65 (s, 1H), 5.60 (s, 2H), 2.41 (s, 3H). HRMS calcd for C₁₈H₁₄N₄O₂S₂ 382.0058, found 382.0059.

N₁-(4-Methyl-1,3-thiazol-2-yl)-2-[1-(3-isopropyl-5-isoxazolyl)methyl]-1H-3-indolyl-2-oxoacetamide (27). Yield: 70%. Yellow solid. ¹H NMR (CDCl₃): δ 9.82 (bs, 1H), 9.03 (s, 1H), 8.47–8.43 (1H, m), 7.41–7.36 (m, 4H), 6.76 (s, 1H), 5.92 (s, 1H), 5.44 (s, 2H), 3.00–2.95 (m, 1H), 2.44 (s, 3H), 1.20 (t, $J = 6.9$ Hz, 6H). ESMS m/z 409.0 (MH⁺).

Acknowledgment. This study was supported by grants BP-090-PP01, BP-090-CF03, and BP-091-CF03 of the National Health Research Institutes, Taiwan, R.O.C. We would like to thank Professor C.-C. Liao of National Tsing Hua University and Dr. Tony C.-C. Liang for helpful comments; Drs. Y. S. Chao and C. M. Chang, and Ms. H. W. Chu and Ms. S. F. Jung, for their administrative support.

References

- Weyand, M.; Schlichting, I. Crystal structure of wild-type tryptophan synthase complexed with the natural substrate indole-3-glycerol phosphate. *Biochemistry* **1999**, *38*, 16469–16480.
- Huber, U.; Moore, R. E.; Patterson, G. M. L. Isolation of a nitrile-containing indole alkaloid from the terrestrial blue-green alga hapalosiphon delicatulus. *J. Nat. Prod.* **1998**, *61*, 1304–1306.
- Skibo, E. B.; King, C.; Dorr, R. T. Aziridinyl quinone antitumor agents based on indoles and cyclopent[*b*]indoles: structure–activity relationships for cytotoxicity and antitumor activity. *J. Med. Chem.* **2001**, *44*, 3545–3562.
- Mewshaw, R. E.; Webb, M. B.; Marquis, K. L.; McGaughey, G. B.; Shi, X.; Wasik, T.; Scerni, R.; Brennan, J. A.; Andree, T. H. New generation dopaminergic agents. 6. Structure–activity relationship studies of a series of 4-(aminoethoxy)indole and 4-(aminoethoxy)indolone derivatives based on the newly discovered 3-hydroxyphenoxyethylamine D2 template. *J. Med. Chem.* **1999**, *42*, 2007–2020.
- Menciu, C.; Duflos, M.; Fouchard, F.; Le Baut, G.; Emig, P.; Achterath, U.; Szelenyi, I.; Nickel, B.; Schmidt, J.; Kutscher, B.; Gunther, E. New *N*-(pyridin-4-yl)-(indol-3-yl)acetamides and propanamides as antiallergic agents. *J. Med. Chem.* **1999**, *42*, 638–648.
- Kalgutkar, A. S.; Marnett, A. B.; Crews, B. C.; Rimmel, R. P.; Marnett, L. J. Ester and amide derivatives of the nonsteroidal antiinflammatory drug, indomethacin, as selective cyclooxygenase-2 inhibitors. *J. Med. Chem.* **2000**, *43*, 2860–2870.
- Kenny, B.; Ballard, S.; Blagg, J.; Fox, D. Pharmacological options in the treatment of benign prostatic hyperplasia. *J. Med. Chem.* **1997**, *40*, 1293–1315.
- Mewshaw, R. E.; Meagher, K. L.; Zhou, P.; Zhou, D.; Shi, X.; Scerni, R.; Smith, D.; Schechter, L. E.; Andree, T. H. Studies toward the discovery of the next generation of antidepressants. Part 2: incorporating a 5-HT(1A) antagonist component into a class of serotonin reuptake inhibitors. *Bioorg. Med. Chem. Lett.* **2002**, *12*, 307–310.
- Bacher, G.; Nickel, B.; Emig, P.; Vanhoefler, U.; Seeber, S.; Shandra, A.; Klenner, T. B.; Beckers, T. D-24851, a novel synthetic microtubule inhibitor, exerts curative antitumoral activity in vivo, shows efficacy toward multidrug-resistant tumor cells, and lacks neurotoxicity. *Cancer Res.* **2001**, *61*, 392–399.
- Schmidt, M.; Lu, Y.; Parant, J.; Lozano, G.; Bacher, G.; Beckers, T.; Fan, Z. Differential roles of p21(Waf1) and p27(Kip1) in modulating chemosensitivity and their possible application in drug discovery studies. *Mol. Pharmacol.* **2001**, *60*, 900–906.
- Bacher, G.; Becker, T.; Emig, P.; Klenner, B.; Kutscher, B.; Nickel, B. New small-molecule tubulin inhibitors. *Pure Appl. Chem.* **2001**, *73*, 1459–1464.
- Simoni, D.; Roberti, M.; Invidiata, F. P.; Rondanin, R.; Baruchello, R.; Malagutti, C.; Mazzali, A.; Rossi, M.; Grimaudo, S.; Capone, F.; Dusonchet, L.; Meli, M.; Raimondi, M. V.; Landino, M.; D'Alessandro, N.; Tolomeo, M.; Arindam, D.; Lu, S.; Benbrook, D. M. Heterocycle-containing retinoids. Discovery of a novel isoxazole arotinoid possessing potent apoptotic activity in multidrug and drug-induced apoptosis-resistant cells. *J. Med. Chem.* **2001**, *44*, 2308–2318.
- Sorgel, F.; Kinzig, M. Pharmacokinetics of gyrase inhibitors. Part 1: Basic chemistry and gastrointestinal disposition. *Am. J. Med.* **1993**, *94*, 44S–55S.
- Hagen, S. E.; Domagala, J.; Gajda, C.; Lovdahl, M.; Tait, B. D.; Wise, E.; Holler, T.; Hupe, D.; Nouhan, C.; Urumov, A.; Zeikus, G.; Zeikus, E.; Lunney, E. A.; Pavlovsky, A.; Gracheck, S. J.; Saunders, J.; VanderRoest, S.; Brodfuehrer, J. 4-Hydroxy-5,6-dihydropyrones as inhibitors of HIV protease: the effect of heterocyclic substituents at C-6 on antiviral potency and pharmacokinetic parameters. *J. Med. Chem.* **2001**, *44*, 2319–2332.
- Chu-Moyer, M. Y.; Ballinger, W. E.; Beebe, D. A.; Berger, R.; Couter, J. B.; Day, W. W.; Li, J.; Mylari, B. L.; Oates, P. J.; Weekly, R. M. Orally effective, long-acting sorbitol dehydrogenase inhibitors: synthesis, structure–activity relationships, and in vivo evaluations of novel heterocycle-substituted piperazopyrimidines. *J. Med. Chem.* **2002**, *45*, 511–528.
- Sauliner, M. G.; Gribble, G. W. Generation and reactions of 3-lithio-1-(phenylsulfonyl)indole. *J. Org. Chem.* **1982**, *47*, 757–761.
- Liu, R.; Zhang, P.; Gan, T.; Cook, J. M. Regiospecific bromination of 3-methylindoles with NBS and its application to the concise synthesis of optically active unusual Tryptophans present in marine cyclic peptides. *J. Org. Chem.* **1997**, *62*, 7447–7456.
- Noyce, D. S.; Fike, S. A. Transmission of substituent effects in heterocyclic systems. Rates of solvolysis of substituted 1-(4-thiazolyl)ethyl chlorides. *J. Org. Chem.* **1973**, *38*, 3321–3324.
- Bergman, J.; Venemalm, L. Acylation of the zinc salt of indole. *Tetrahedron* **1990**, *46*, 6061–6066.
- Yang, C. X.; Patel, H. H.; Ku, Y.-Y.; Shah, R.; Sawick, D. The use of Lewis acid in the reaction of zinc salts of indoles and acyl chloride. *Synth. Commun.* **1997**, *27*, 2125–2132.
- Lautens, M.; Fillion, E. An expedient route for the stereoselective construction of bridged polyheterocyclic ring systems using the tandem “pincer” Diels–Alder reaction. *J. Org. Chem.* **1997**, *62*, 4418–4427.
- Chaudhari, S. S.; Akamanchi, K. G. Thionyl chloride-benzotriazole in methylene chloride: A convenient solution for conversion of alcohols and carboxylic acids expeditiously into alkyl chlorides and acid chlorides by simple titration. *Synlett.* **1999**, *11*, 1763–1765.
- Berry, J. M.; Watson, C. Y.; Whish, J. D.; Threadgill, D. 5-Nitrofuranyl-2-ylmethyl group as a potential bioreductively activated pro-drug system. *J. Chem. Soc., Perkin Trans. 1* **1997**, *8*, 1147–1156.
- Lee, G. A. simplified synthesis of unsaturated nitrogen-heterocycles using nitrile betaines. *Synthesis* **1982**, 508–509.
- Okauchi, T.; Itonaga, M.; Minami, T.; Owa, T.; Kitoh, K.; Yoshino, H. A general method for acylation of indoles at the 3-position with acyl chlorides in the presence of dialkylaluminum chloride. *Org. Lett.* **2000**, *10*, 1485–1487.
- Ottoni, O.; Neder, A. de V. F.; Dias, A. K. B.; Cruz, R. P. A.; Aquino, L. B. Acylation of indole under Friedel–Crafts conditions – an improved method to obtain 3-acylindoles regioselectively. *Org. Lett.* **2001**, *3*, 1005–1008.
- Goodwin, C. J.; Holt, S. J.; Downes, S.; Marshall, N. J. Microculture tetrazolium assays: a comparison between two new tetrazolium salts, XTT and MTS. *J. Immunol. Methods* **1995**, *179*, 95–103.
- Communal, C.; Singh, K.; Pimentel, D. R.; Colucci, W. S. Norepinephrine stimulates apoptosis in adult rat ventricular myocytes by activation of the beta-adrenergic pathway. *Circulation* **1998**, *98*, 1329–1334.

- (29) Rose, W. C.; Basler, G. A.; Trail, P. A.; Saulnier, M.; Crosswell, A. R.; Casazza, A. M. Preclinical antitumor activity of a soluble etoposide analogue, BMY-40481–30. *Invest. New Drugs* **1990**, *8 Suppl 1*, S25–S32.
- (30) Ghose, A. K.; Viswanadhan, V. N.; Wendoloski, J. J. Prediction of hydrophobic (lipophilic) properties of small organic molecules using fragmental methods: An analysis of ALOGP and CLOGP methods. *J. Phys. Chem. A* **1998**, *102*, 3762–3772.
- (31) Sparreboom, A.; van Asperen, J.; Mayer, U.; Schinkel, A. H.; Smit, J. W.; Meijer, D. K.; Borst, P.; Nooijen, W. J.; Beijnen, J. H.; van Tellingen, O. Limited oral bioavailability and active epithelial excretion of paclitaxel (Taxol) caused by P-glycoprotein in the intestine. *Proc. Natl. Acad. Sci. U.S.A.* **1997**, *94*, 2031–2035.
- (32) Kimura, Y.; Aoki, J.; Kohno, M.; Ooka, H.; Tsuruo, T.; Nakanishi, O. P-glycoprotein inhibition by the multidrug resistance-reversing agent MS-209 enhances bioavailability and antitumor efficacy of orally administered paclitaxel. *Cancer Chemother. Pharmacol.* **2002**, *49*, 322–328.
- (33) van Asperen, J.; van Tellingen, O.; Sparreboom, A.; Schinkel, A. H.; Borst, P.; Nooijen, W. J.; Beijnen, J. H. Enhanced oral bioavailability of paclitaxel in mice treated with the P-glycoprotein blocker SDZ PSC 833. *Br. J. Cancer.* **1997**, *76*, 1181–1183.

JM020471R